Catalysis
Science & Technology

RSC Publishing

PAPER

View Article Online
View Journal

Cite this: DOI: 10.1039/c3cy00082f

Preparation of carbon nanotube-supported α-Fe_2O_3@CuO nanocomposite: a highly efficient and magnetically separable catalyst in cross-coupling of aryl halides with phenols†

Dariush Saberi,[a] Mehdi Sheykhan,[b] Khodabakhsh Niknam[c] and Akbar Heydari*[a]

Herein, we introduce the first magnetic CuO nanoparticles based on carbon nanotubes as a highly intriguing magnetic catalyst in Ullmann-type coupling of aryl halides with phenols. Two facile procedures were used for the preparation of this magnetically separable catalytic system. Having been treated with $FeSO_4$ and then H_2O_2, nanotubes accommodated the resulting iron hydroxides on the walls. The resulting nanocomposite was then exposed to argon atmosphere at 450 °C giving rise to a carbon nanotube-supported α-Fe_2O_3 compound. Ultimately, copper acetate was hydrolysed in the presence of CNT supported α-Fe_2O_3 at 100 °C and our novel catalyst was gained. Some spectroscopic and microscopic techniques such as Infrared spectroscopy (IR), X-ray diffraction spectroscopy (XRD), Vibrational sample magnetometry (VSM), Brunauer–Emmett–Teller (BET), Barrett–Joyner–Halenda (BJH), Inductively coupled plasma (ICP), Scanning electron microscopy (SEM) and Transmission electron microscopy (TEM) corroborated the structure of the catalyst. The catalyst synthesized showed good activity in C–O cross coupling reactions affording the highest rate of completion. Magnetic feature of the catalyst helped facile separation of it from the reaction medium. The catalyst could also be reused up to six times without any loss of its activity.

Received 3rd February 2013,
Accepted 2nd April 2013

DOI: 10.1039/c3cy00082f

www.rsc.org/catalysis

Introduction

Aryl ethers play a significant role as building blocks in a wide range of natural products[1] and various pharmaceuticals with antibiotic activity, such as antitumoral bouvardin,[2] antiviral peptide K-13[3] and vancomycin.[4] One of the most popular methods for synthesis of aryl ethers is the Ullmann-type coupling reaction[5] (copper-catalyzed cross-couplings of aryl halides with phenols). On account of the problems associated with this noteworthy reaction such as long reaction time, high temperature (>200 °C) and stoichiometric amount of copper required as catalyst, organic chemists made persevering efforts to set the stage for satisfactory reaction conditions to overcome this downside and fortunately success was achieved in this area. Buchwald and Hartwig, pioneers of C–O cross-couplings based on Ullmann method, reported palladium-catalyzed coupling reactions using phosphine ligands for the synthesis of aryl ethers.[6] Nevertheless, the use of expensive palladium as well as air and moisture sensitive phosphine ligands are some drawbacks of this method for large-scale or industrial applications. Consequently, attempts were directed to improve the strict conditions of copper-catalyzed C–O coupling reactions. In 1997 Buchwald *et al.* reported the first examples of copper-catalyzed synthesis of diaryl ethers by the reaction of aryl bromides or aryl iodides with phenols using $Cu(OTf)_2$.PhH as the catalyst and Cs_2CO_3 as the base in toluene.[7]

Thereafter, it was found that exploiting additives such as *N,N*-dimethylglycine,[8] 1,1,1-tris(hydroxymethyl)ethane,[9] pyrrolidine-2-phosphonic acid phenyl monoester,[10] 1,10-phenanthroline,[11] neocuproine,[12] 2,2,6,6-tetramethylheptane-3,5-dione,[13] or β-keto ester[14] resulted in milder conditions, that is, somewhat boosted reaction rates, diminished amount of catalyst needed and lower temperatures. Moreover, Bolm *et al.* reported the Ullmann-type coupling reactions with part-per-million catalyst loading in the presence of $FeCl_3$ as a low-cost and environmentally green catalyst.[15] In recent years, magnetic nanoparticles have been

[a] Chemistry Department, Tarbiat Modares University, P.O. Box 14155-4838, Tehran, Iran. E-mail: heydar_a@modares.ac.ir; Fax: +98-21-82883455; Tel: +98-21-82883444
[b] Chemistry Department, Guilan University, P.O. Box 41335-1914, Rasht, Iran
[c] Chemistry Department, Faculty of Sciences, Persian Gulf University, Bushehr, 75169, Iran

† Electronic supplementary information (ESI) is available. See DOI: 10.1039/c3cy00082f

used for the C–O coupling reactions as both support and catalyst.[16] Nevertheless, the reaction conditions did not gain the chemists' full satisfaction. Therefore, there have remained endeavours to reach more favourable conditions. In this regard, using supports to put the catalyst on is one of the measures taken to alleviate these strenuous conditions. Today, utility of a platform leading to heterogeneous catalytic systems especially when a toxic and costly transition metal is exploited as the catalyst, has warranted attention since it provides recovery and reusability of the catalyst which is desirable from economical and environmental point of view. In this context, metal oxides (silica, alumina and *etc.*), various kinds of polymers, zeolites, carbon active and carbon nanotubes[17] are typical supports that have recently been used in most catalytic systems.[18] Among them, carbon nanotubes due to their unique features such as large specific surface area (stemming from their hollow geometries), high oxidation stability (induced by their structural integrity and chemical inertia) and significant mechanical and thermal stability, have taken up a specific position in industry and academia.[19]

Bear in mind that nano-sized materials have distinguished hallmark of having high surface area, which is a virtue accounting for various applications of such compounds. In the case of a nano-sized catalyst, this feature enhances the catalytic activity *via* increasing its active sites. On the other hand, nano-sized catalyst would be more dispersed in solution, hence forming an emulsion which imposes difficulty in catalyst separation from the reaction media. However, in this extreme case of immobilized systems, too, the same problems of isolation and recycling of homogeneous catalysts would be encountered. To circumvent these problems, one solution is to employ magnetic nanoparticles. One drastic impact that such particles possess is that by applying an external magnetic field, they can be dispersed or aggregated which allows for the facile separation and recycling of immobilized catalysts on the nano-sized supports. Lately, magnetic nanoparticles have found use as both catalyst and support.[20] In this paper and in pursuit of our interests in the preparation and application of heterogeneous catalytic systems based on magnetic nanoparticles in organic reactions,[21] we succeeded in innovating a new catalytic system consisting of copper oxide nanoparticles supported on carbon nanotube modified by iron oxide (CNT@α-Fe_2O_3@CuO) as a highly efficient and magnetically separable catalyst in C–O coupling of aryl halides with phenols. This catalytic system is easily prepared and shows good catalytic activity along with the straightforward separation from reaction media. Although, the conditions utilized in this reaction are not extremely gentle, it provides a remarkably reduced reaction time in comparison to the previous reports. Presumably, it is because of the high degree of nanoparticles' dispersion on the walls of the CNTs.

Results and discussion

New catalytic system was prepared according to the following procedures. Carbon nanotubes were decorated by α-Fe_2O_3 after being exposed to $FeSO_4$–H_2O_2 followed by heating at 450 °C under argon atmosphere.[22] Having completed the first stage we moved on to step 2 in which copper acetate was hydrolysed in the presence of CNT@α-Fe_2O_3 and our catalytic system was generated.[23]

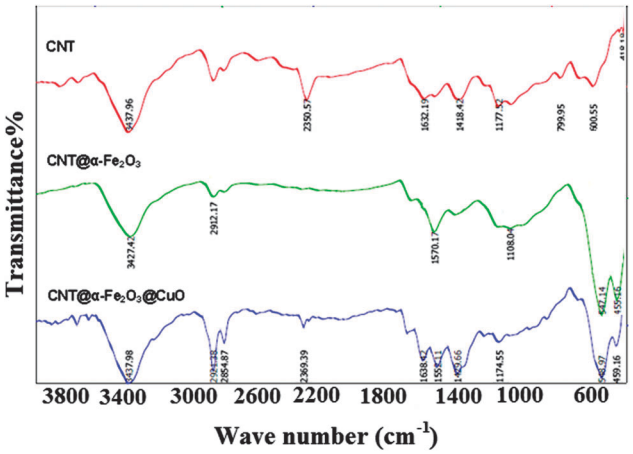

Fig. 1 FT-IR spectra of raw CNT, CNT@α-Fe_2O_3, CNT@α-Fe_2O_3@CuO.

The prepared catalyst was well characterized by the following instrumental techniques: FT-IR, XRD, VSM, BET, BJH, ICP, SEM and TEM.

The FT-IR spectra of raw CNT, CNT@α-Fe_2O_3 and CNT@α-Fe_2O_3@CuO have been shown in Fig. 1. The broad band at over 3400 cm^{-1} corresponds to the stretching vibrations of hydroxyl groups on the external surface of the CNTs. In addition, the band can also be attributed to hydroxyl groups of the physically adsorbed water. The signal at 2900 cm^{-1} is relevant to C–H bond stretching vibrations. The signals related to stretching vibrations of C=C bond are located within 1400–1600 cm^{-1}. The band emerged at 1174 cm^{-1} is assigned to stretching vibrations of C–O bond. All the above-mentioned signals are typical of the skeleton of carbon nanotubes. The appearance of a strong peak at 400–600 cm^{-1} in the IR spectra of CNT@α-Fe_2O_3 and CNT@α-Fe_2O_3@CuO implies the formation of new phases on carbon nanotubes. These peaks are ascribed to stretching vibrations of Fe–O and Cu–O bonds.[19b]

The crystalline structure of catalyst was characterized by XRD. As shown in Fig. 2, the patterns can be readily referred to hematite (JCPDS no. 33-0664), tenorite (JCPDS no. 48-1548) and graphite (JCPDS no. 12-0212). In the pattern assigned to hematite, diffraction peaks at around 24.1°, 33.2°, 35.8°, 40.9°, 49.5°, 54.1°, 57.5°, 57.6° , 62.4° and 64.0° correspond to the (012), (104), (110), (113), (024), (116), (122), (018), (214) and (300) reflections, respectively. For tenorite, diffraction peaks at around 35.7°, 38.8°, 67.9° and 68.2° are attributable to the (−111), (111), (022) and (311) reflections, respectively. Diffraction peak at 26.4° can be indexed to (022) reflection of the CNTs. No other characteristic peaks due to the impurities of other oxides of iron and copper were detected. The large peak widths are ascribed to the formation of nanosized particles of CuO. The size of particles were calculated by Debye–Scherrer equation[24] using the (−111) peak (2θ = 35.5°) which is 20.9 nm.

Superparamagnetic feature of the catalyst which caused its easy recovery, was confirmed by vibrating sample magnetometery

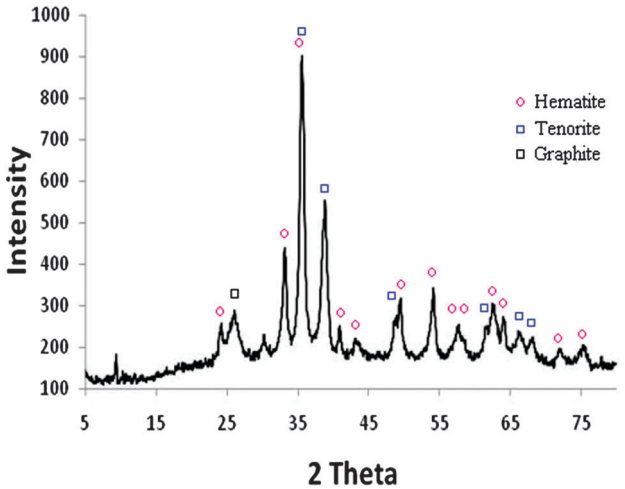

Fig. 2 XRD pattern of CNT@α-Fe_2O_3@CuO.

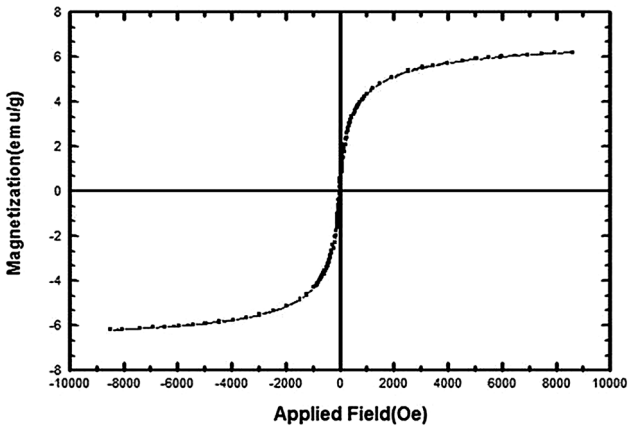

Fig. 3 Magnetization curve of CNT@α-Fe_2O_3@CuO.

analysis (there is no hysteresis loop and the ratio of magnetic remanence/magnetic saturation (M_s) is about 0.0004, M_s = 6.0 emu g^{-1}). Magnetization curve of the catalyst is depicted in Fig. 3.

The surface morphologies of prepared CNT@α-Fe_2O_3 and CNT@α-Fe_2O_3@CuO were investigated by SEM and the micrographs have been outlined in Fig. 4 which bears out coating of new phases on CNTs.

The porous nature of α-Fe_2O_3@CuO nanoparticles were clearly proved by the BJH method. A type-IV hysteresis loop was detected which clearly displayed two peaks with the pore size centred at about 2.7 nm and 12.2 nm, respectively, for two types of pores. The increased active site of the CNT@α-Fe_2O_3@CuO nanocomposite was studied by the nitrogen adsorption–desorption isotherms from the BET analysis. The specific surface area and pore volume of the mesoporous catalyst were calculated as 112.6 $m^2 g^{-1}$ and 0.66 $cm^3 g^{-1}$, respectively. From the adsorption branch of the isotherms, the narrow pore size calculated was gained about 1.6 nm. (Fig. 5).

The copper content in CNT@α-Fe_2O_3@CuO catalyst was measured by ICP instrument. To conduct this analysis, the catalyst was dissolved in a mixture of nitric acid and

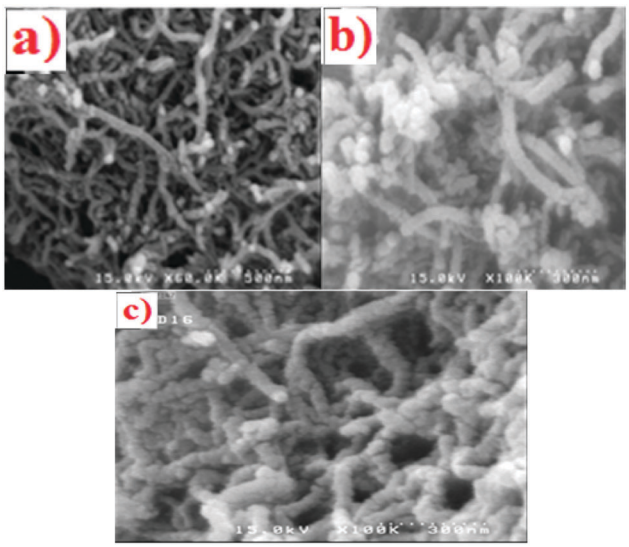

Fig. 4 SEM micrographs of (a) raw CNT; (b) CNT@α-Fe_2O_3 and (c) CNT@α-Fe_2O_3@CuO.

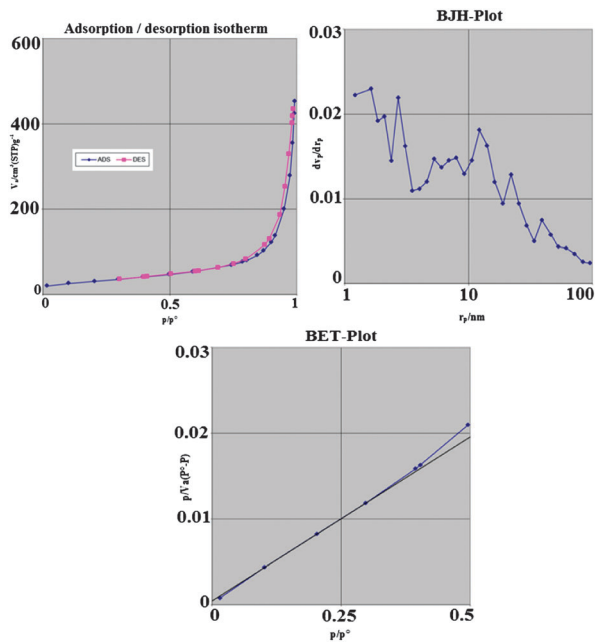

Fig. 5 N_2 adsorption–desorption analysis, Brunauer–Emmett–Teller (BET) analysis and Barrett–Joyner–Halenda (BJH) analyseis of CNT@α-Fe_2O_3@CuO.

hydrochloric acid to digest the copper oxide. In the end, copper content of the catalyst was obtained 1.85 mmol g^{-1}.

TEM images of raw CNT, CNT@α-Fe_2O_3 and CNT@α-Fe_2O_3@CuO are shown in Fig. 6. Congestion of nanoparticles which can be seen on the external walls of CNTs is representative of the formation of new phases.

After characterization of catalyst, its catalytic activity was tested in cross-coupling of aryl halides with phenols. As a model study for the optimization of the reaction, the iodobenzene (0.5 equiv.) was treated with phenol (1 equiv.) in the presence of CNT@α-Fe_2O_3@CuO (10 mg, 1.85 mol% CuO) (Scheme 1).

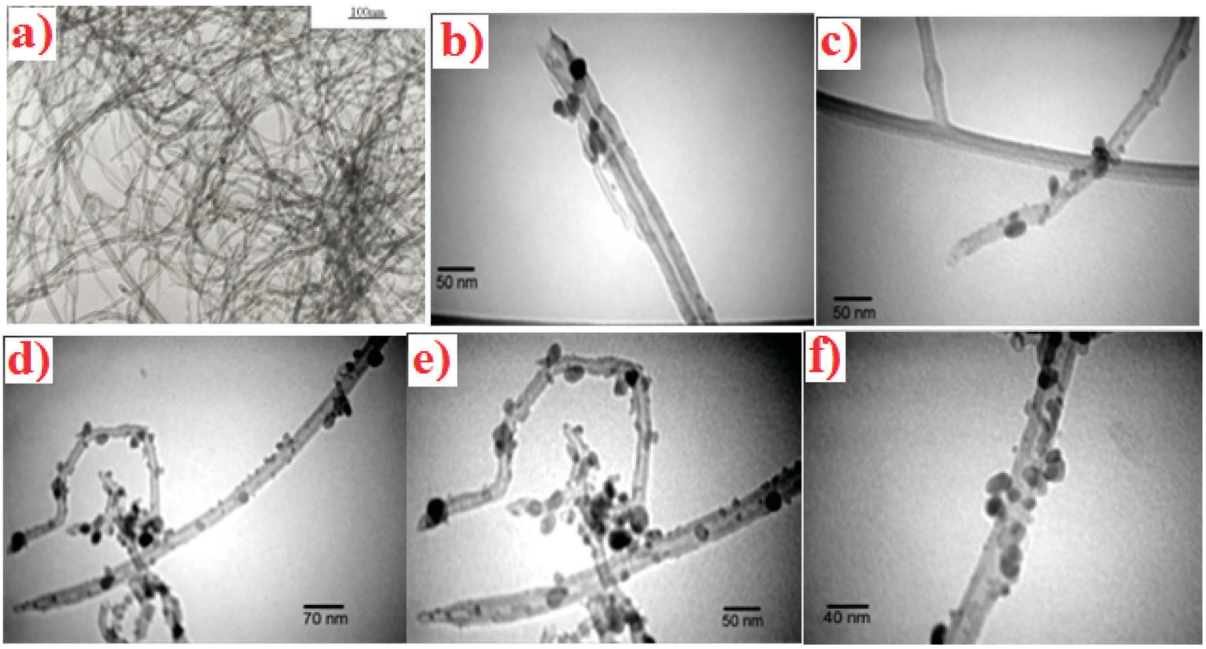

Fig. 6 TEM micrographs of (a) raw CNT; (b and c) CNT@α-Fe_2O_3 and (d–f) CNT@α-Fe_2O_3@CuO.

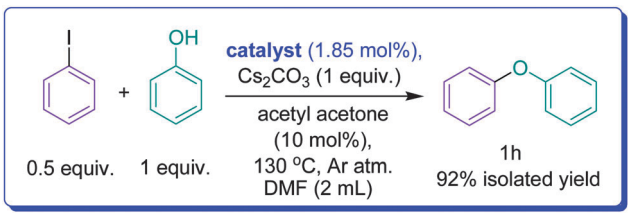

Scheme 1 Devising the first magnetic carbon nanotube coated CuO nanoparticles for diaryl coupling.

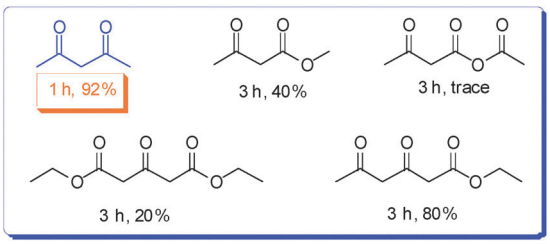

Scheme 2 Influence of different 1,3-dicarbonyl compounds as ligands in coupling reaction of iodobenzene (0.5 mmol) with phenol (1 mmol) with following conditions: DMF (2 mL), catalyst (10 mg), ligand (10 mol%), 130 °C under argon atmosphere.

The reaction conditions were optimized by taking into consideration parameters such as ligand, solvent, base, and amount of catalyst (Table 1). The influence of DMF, toluene and DMSO as solvents on the yield of the reaction was examined and DMF was chosen as the most efficient solvent. Different bases (K_2CO_3, Cs_2CO_3, Na_2CO_3, NaOH and ^{t}BuOK) were used in the model reaction and Cs_2CO_3 proved to be superior to all other choices. Additionally, the role of ligand was assessed by conducting the reaction in its absence. Under these conditions, the reaction proceeded far more slowly. During the preliminary studies, miscellaneous assortments of 1,3-dicarbonyl compounds as ligands were screened and acetyl acetone afforded the best yields of diaryl ethers (Scheme 2).

Table 1 Study of some parameters on model reaction[a]

Entry	Solvent	Base	Temp. (°C)	Time (h)	Yield (%)
1	DMF	Cs_2CO_3	130	1	92
2	DMF	KOt-Bu	130	2	75
3	DMF	K_2CO_3	130	3	60
4	DMF	Na_2CO_3	130	3	30
5	DMF	NaOH	130	3	60
6	Toluene	Cs_2CO_3	130	4	NR
7	DMSO	Cs_2CO_3	130	1	80
8	DMF	Cs_2CO_3	110	1	72
9	DMF	Cs_2CO_3	90	1	40
10	DMF	Cs_2CO_3	90	10	90
11	DMF	Cs_2CO_3	130	1	93[b]
12	DMF	Cs_2CO_3	130	1	60[c]

[a] Reaction condition: iodobenzene (0.5 mmol), phenol (1 mmol), catalyst (10 mg), base (2 equiv.), solvent (2 mL), acetyl acetone (10 mol%), under Ar atm. [b] 15 mg of catalyst was used. [c] 5 mg of catalyst was used.

The effect of temperature was also investigated. It was found that raising the reaction temperature from 90 to 130 °C resulted in a drastic improvement in the yield. Also prolonging the reaction time even at 90 °C rose the yield from 40 to 90% (Table 1, entry 10). All reactions were performed under argon atmosphere.

In the presence of CNT@α-Fe_2O_3 (without CuO loading) as catalyst only 30% of starting materials was converted to the product after 24 h. The reaction was repeated using CNT@CuO as catalyst. Although, the results were similar to CNT@α-Fe_2O_3@CuO but the easy magnetic recovery was lost.

Eventually, the coupling reaction between phenols and aryl iodides and bromides was studied in the presence of CNT supported α-Fe_2O_3@CuO nanoparticles acting as the heterogeneous catalyst as well as Cs_2CO_3 as the base and DMF as the solvent at 130 °C under argon atmosphere.

Motivated by the profound change brought about in the rate of reactions of choice by utilizing CNT supported α-Fe_2O_3@CuO, we extended the scope of the C–O coupling reactions using this novel catalyst and exploited various phenols to treat with some other derivatives of iodo and bromo benzenes (Table 2). Generally speaking, the reactions were performed both faster and cleaner than all other C–O cross coupling reactions ever reported. As is seen in Table 2, besides aryl iodides, less reactive aryl bromides can be efficiently coupled with phenol derivatives. The effects of various substituents on each reagent were explored. As expected, the presence of electron withdrawing groups on the phenol moiety (Table 2, entry 3) decreases the yield of the product, plus prolonging the reaction time tangibly. In contrast, electron-releasing groups such as methoxy and methyl on phenol enhance the yield of the reaction (Table 2, entry 2, 4, 6 and 7). In comparison, electron donating groups on aryl halide give rise to the same effects as electron withdrawing groups on the phenol (Table 2, entry 13) contrary to electron-withdrawing group which cause the reaction to proceed even without CNT@α-Fe_2O_3@CuO (Table 2, entry 14). These findings denote that the latter reaction is performed through a nucleophilic addition-elimination mechanism rather than a copper oxide catalyzed coupling reaction as was reported previously.[25]

Needless to say that chlorobenzene and its derivatives have the least reactivity among aryl halides in the coupling reactions. Thus, in this special reaction, even using our catalytic system led to only a trace of product when chlorobenzene and phenol reacted with one another, (Table 2, entry 1).

Having assessed most facets of our catalyst, now it was time to examine another overriding attribute of it. Undoubtedly, one of the main criteria in the evaluation of a catalyst especially from an industrial standpoint is its lifetime. Leaching process is one of the factors that affect longevity of the catalyst substantially. To vindicate that our reaction does not suffer from leaching process, confirmation of the heterogeneous nature of the catalyst in the model reaction was achieved by a decantation experiment, in which the reaction mixture was decanted using a magnet after 30 min (50% conversion). No catalytic activity was observed in the filtrate during 6 h after the filtration. To rule out the deactivation of catalyst, its efficient recovery was accomplished by decantation of the reaction mixture using an external magnet and the recovered catalyst was successively used in a second run. When the reaction time was set to 1 h, comparably excellent yields were obtained in six subsequent runs using the same catalyst with only a negligible decrease of its aptitude (Fig. 7).

The efficacy of the CuO nanoparticles supported on magnetic CNTs in comparison with some previously reported catalysts including supported and unsupported copper source is illustrated in Table 3. As can be seen, our catalytic system performs the reaction at the highest rate. Clearly, it is this decreased reaction time that provides such high turnover frequency.

Table 2 Diversity of CNT@α-Fe_2O_3@CuOcatalyzed C–O cross coupling reaction[a]

Entry	Aryl halide	Phenol	Product	Time (h)	Yield[b] (%)
1	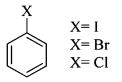 X= I, X= Br, X= Cl		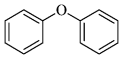	1 4 10	92 95 Trace
2	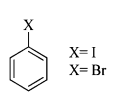 X= I, X= Br	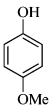	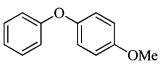	1 2	90 85
3	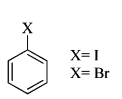 X= I, X= Br	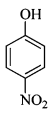	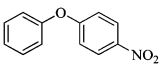	10 10	50 45
4	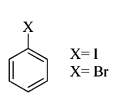 X= I, X= Br	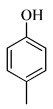	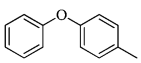	2 4	95 95
5	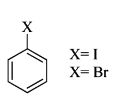 X= I, X= Br	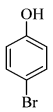	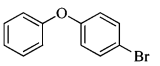	5 5	60 40
6	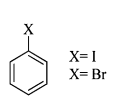 X= I, X= Br	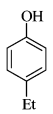	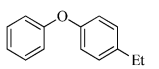	2 2.5	90 93
7	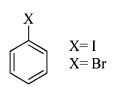 X= I, X= Br		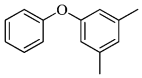	1 2	85 85
8	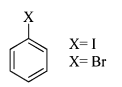 X= I, X= Br	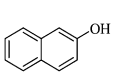	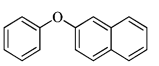	1	95
9	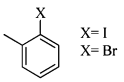 X= I, X= Br		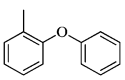	3 4 5	90 70 70
10			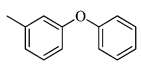	5	72
11	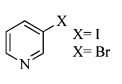 X= I, X= Br		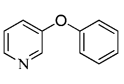	7 7	75 70
12	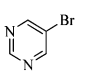		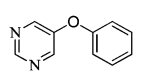	3	78
13	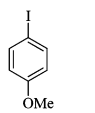	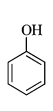	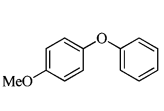	8	70
14	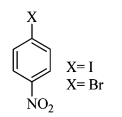 X= I, X= Br			0.5 0.5	96[c] 95[c]

[a] Reaction conditions: aryl halide (0.5 equiv.), phenol (1 equiv.), catalyst (10 mg), DMF (2 mL), Cs_2CO_3 (1 equiv.), acetyl acetone (10 mol%), under Ar atmosphere. [b] Isolated yield. [c] Without catalyst.

Conclusion

We developed a novel and alternative route to catalyse C–O cross couplings. To this end, carbon nanotube-supported α-Fe_2O_3@CuO

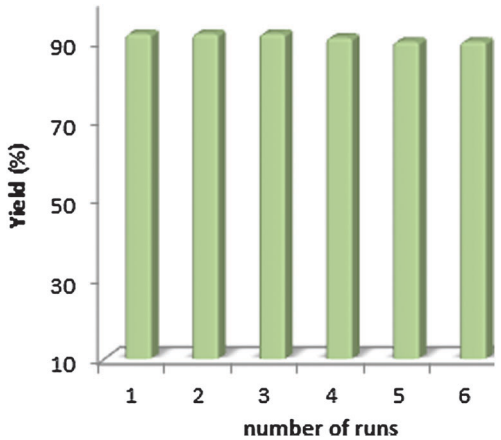

Fig. 7 Reusability of CNT@α-Fe_2O_3@CuO in reaction between iodobenzene and phenol.

Table 3 Comparison of different catalysts in *O*-arylation reaction between iodobenzene and phenol[a]

Entry	Catalyst	Time (h)	Yield (%)	Ref.	TOF (h^{-1})
1	CuO nanoparticles	15	93	26	2.48
2	CuI	15	95	27	0.63
3	Cu_2O	24	93	28	3.87
4	CuBr	20	97	29	0.48
5	Polymer-$Cu(Oac)_2$	12	95	30	3.04
6	$CuFe_2O_4$[b]	24	84	31	0.175
7	CuO	24	87	15	36.25
8	CuO/γ-Al_2O_3[c]	10	76	32	0.038
9	CuO/SBA-15[c]	10	8	32	0.004
10	CNT@α-Fe_2O_3@CuO	1	92	**Present work**	49.73

[a] Condition: base/solvent/temp. For entries: (1) KOH/DMSO/110 °C; (2) Cs_2CO_3/DMF/110 °C; (3) Cs_2CO_3/CH_3CN/80 °C; (4) Cs_2CO_3/DMSO/60 °C; (5) Cs_2CO_3/DMSO/120 °C; (6) Cs_2CO_3/DMF/135 °C; (7) Cs_2CO_3/toluene/135 °C; (8) K_3PO_4/DMSO/150 °C; (9) K_3PO_4/DMSO/150 °C (10) Cs_2CO_3/DMF/130 °C. [b] 4-Methyliodobenzene has compared instead of iodobenzene. [c] 3-Methyl phenol has compared instead of phenol.

was prepared and its catalytic activity was explored in Ullmann-type coupling of aryl iodides and bromides with phenols. As a result, the time of the reaction was reduced tremendously. Reduction in time causes a high TOF. Facile preparation, straightforward separation, remarkable aptitude to be recycled up to six times and good stability are all salient features of this catalytic system.

Experimental section

General procedure for the *O*-arylation of phenols

A mixture of aryl halide (0.5 equiv.), phenol (1.0 equiv.), Cs_2CO_3 (1.0 equiv.), CNT@α-Fe_2O_3@CuO (10 mg, 1.85 mol%), acetylacetone (10 mol%), and DMF (2 mL) in a two-necked flask was heated at 130 °C under argon atmosphere for a specified time. The cooled mixture was partitioned between ethyl acetate and water. The organic layer was separated, and the aqueous layer was extracted with ethyl acetate. The combined organic layers were dried over Na_2SO_4, and concentrated to yield product, which was purified by silica gel chromatography to produce the corresponding diaryl ether.

Acknowledgements

We are thankful to Tarbiat Modares University for partial support of this work and the University of Manchester for taking the ^1H NMR and ^{13}C NMR of some compounds.

Notes and references

1 K. C. Nicolau, C. N. C. Boddy, S. Brase and N. Winssinger, *Angew. Chem., Int. Ed.*, 1999, **38**, 2096–2152.
2 D. L. Boger, M. A. Patane and J. Zhou, *J. Am. Chem. Soc.*, 1994, **116**, 8544–8556.
3 J. W. Janetka and D. H. Rich, *J. Am. Chem. Soc.*, 1997, **119**, 6488–6495.
4 K. C. Nicolaou and C. N. C Boddy, *J. Am. Chem. Soc.*, 2002, **124**, 10451–10455.
5 F. Ullmann, *Ber. Dtsch. Chem. Ges.*, 1904, **37**, 853–857; F. Ullmann, *Ber. Dtsch. Chem. Ges.*, 1903, **36**, 2382–2384.
6 G. Mann and J. F. Hartwig, *Tetrahedron Lett.*, 1997, **46**, 8005–8008; M. Palucki, J. P. Wolfe and S. L. Bukhwald, *J. Am. Chem. Soc.*, 1996, **118**, 10333–10334; G. Mann and J. F. Hartwig, *J. Am. Chem. Soc.*, 1996, **118**, 13109–13110; A. Aranyos, D. W. Old, A. Kiyomori, J. P. Wolfe, J. P. Sadighi and S. L. Buchwald, *J. Am. Chem. Soc.*, 1999, **121**, 4369–4378; G. Mann and J. F. Hartwig, *J. Org. Chem.*, 1997, **62**, 5413–5418; M. Palucki, J. P. Wolfe and S. Buchwald, *J. Am. Chem. Soc.*, 1997, **119**, 3395–3396; R. A. Widenhoefer, H. A. Zhong and S. L. Buchwald, *J. Am. Chem. Soc.*, 1997, **119**, 6787–6795.
7 J. F. Marcoux, S. Doye and S. L. Buchwald, *J. Am. Chem. Soc.*, 1997, **119**, 10539–10540.
8 D. Ma and Q. Cai, *Org. Lett.*, 2003, **5**, 3799–3802.
9 Y. J. Chen and H. H. Chen, *Org. Lett.*, 2006, **8**, 5609–5612.
10 H. Rao, Y. Jin, H. Fu, Y. Jiang and Y. Zhao, *Chem.–Eur. J.*, 2006, **12**, 3636–3646.
11 M. Wolter, G. Nordmann, G. E. Job and S. L. Buchwald, *Org. Lett.*, 2002, **4**, 973–976.
12 R. K. Gujadhur, C. G. Bates and D. Venkataraman, *Org. Lett.*, 2001, **3**, 4315–4317.
13 E. Buck, Z. J. Song, D. Tschaen, P. G. Dormer, R. P. Volante and P. J. Reider, *Org. Lett.*, 2002, **4**, 1623–1626.
14 X. Lv and W. Bao, *J. Org. Chem.*, 2007, **72**, 3863–3867.
15 S. L. Buchwald and C. Bolm, *Angew. Chem., Int. Ed.*, 2009, **48**, 5586–5587; P. F. Larsson, A. Correa, M. Carril, P. O. Norrby and C. Bolm, *Angew. Chem., Int. Ed.*, 2009, **48**, 5691–5693; O. Bistri, A. Correa and C. Bolm, *Angew. Chem., Int. Ed.*, 2008, **47**, 586–588.
16 R. Arundhathi, D. Damodara, P. R. Likhar, M. L. Kantam, P. Saravanan, T. Magdaleno and S. H. Kwon, *Adv. Synth. Catal.*, 2011, **353**, 2875–2883; S. Yang, C. Wu, H. Zhou, Y. Yang, Y. Zhao, C. Wang, W. Yang and J. Xu, *Adv. Synth. Catal.*, 2013, **355**, 53–58.
17 S. Iijima, *Nature*, 1991, **354**, 56–58.

18 T. Miao and L. Wang, *Tetrahedron Lett.*, 2007, **48**, 95–99; S. M. Islam, S. Mondal, P. Mondal, A. S. Roy, K. Tuhina, N. Salam and M. Mobarak, *J. Organomet. Chem.*, 2012, **696**, 4264–4274; P. Ling, D. Li and X. Wang, *J. Mol. Catal. A: Chem.*, 2012, **357**, 112–116; M. Islam, S. Mondal, P. Mondal, A. S. Roy, D. Hossain and M. Mobarak, *Transition Met. Chem.*, 2011, **36**, 1–11; G. M. Neelgund and A. Oki, *Appl. Catal., A*, 2011, **399**, 154–160; A. Corma, H. Garcia and A. Leyva, *J. Mol. Catal. A: Chem.*, 2005, **230**, 97–105; J. M. Planeix, N. Coustel, B. Coq, V. Bretons, P. S. Kumbhar, R. Dutartre, P. Geneste, P. Bernier and P. M. Ajayan, *J. Am. Chem. Soc.*, 1994, **116**, 7935–7936; V. G. Ramu, A. Bordoloi, T. C. Nagaiah, W. Schuhmann, M. Muhler and C. Cabrele, *Appl. Catal., A*, 2012, **431–432**, 88–94; S. M. Chergui, A. Ledebt, F. Mammeri, F. Herbst, B. Carbonnier, H. B. Romdhane, M. Delamar and M. M. Chehimi, *Langmuir*, 2010, **26**, 16115–16121; S. Heylen, N. Delcour, C. E. A. Kirschhock and J. A. Martens, *ChemCatChem*, 2012, **4**, 1162–1166; J. Wang, F. Zhang, W. Hua, Y. Yue and Z. Gao, *Catal. Commun.*, 2012, **18**, 63–67.

19 P. G. F. Harris, *Carbon Nanotubes and Related Structures*, Cambridge University Press, Cambridge, UK, 2003; *Carbon Nanotubes: Synthesis, Structure, Properties, and Applications*, ed. M. S. Dresselhaus, G. Dresselhaus and P. Avouris, Springer, New York, 2000; R. Saito, G. Dresselhaus and M. S. Dresselhaus, *Physical Properties of Carbon Nanotubes*, Imperial College Press, London, 1998; P. M. Ajayan, *Chem. Rev.*, 1999, **99**, 1787–1799; M. Terrones, *Annu. Rev. Mater. Res.*, 2003, **33**, 419–501; M. S. Dresselhaus, G. Dresselhaus, J. C. Charlier and E. Hernandez, *Philos. Trans. R. Soc. London, Ser. A*, 2004, **362**, 2065–2098.

20 R. A. Reziq, H. Alper, D. Wang and M. L. Post, *J. Am. Chem. Soc.*, 2006, **128**, 5279–5283; A. Hu, T. Gordon, G. T. Yee and W. Lin, *J. Am. Chem. Soc.*, 2005, **127**, 12486–12487; P. D. Stevhens, G. Li, J. Fan, M. Yen and Y. Gao, *Chem. Commun.*, 2005, 4435–4437; P. D. Stevens, J. Fan, H. M. R. Gardimalla, M. Yen and Y. Gao, *Org. Lett.*, 2005, **7**, 2085–2088; D. Lee, J. Lee, H. Lee, S. Jin, T. Hyeon and B. M. Kim, *Adv. Synth. Catal.*, 2006, **348**, 41–46; S. Luo, X. Zheng, H. Xu, X. Me, L. Zhang and J. P. Cheng, *Adv. Synth. Catal.*, 2007, **349**, 2431–2434; H. Firouzabadi, N. Iranpoor, M. Gholinejad and J. Hoseini, *Adv. Synth. Catal.*, 2011, **353**, 125–132.

21 M. Sheykhan, L. Ma'mani, A. Ebrahimi and A. Heydari, *J. Mol. Catal. A: Chem.*, 2011, **335**, 253–261; L. Ma'mani, M. Sheykhan and A. Heydari, *Appl. Catal., A*, 2011, **395**, 34–38; L. Ma'mani, A. Heydari and M. Sheykhan, *Appl. Catal., A*, 2010, **384**, 122–127.

22 P. Feng, F. Xiao-Bo, Y. Hao and W. Hong-juan, *New Carbon Mater.*, 2007, **22**, 213–217.

23 J. Zhu, H. Bi, Y. Wang, X. Wang, X. Yang and L. Lu, *New Carbon Mater.*, 2007, **61**, 5236–5238.

24 N. A. Smith, N. Sekido, J. H. Perepezko, A. B. Ellis and W. C. Crone, *Scr. Mater.*, 2004, **51**, 423–426.

25 A. B. Naidu, E. A. Jaseer and G. Sekar, *J. Org. Chem.*, 2009, **74**, 3675–3679.

26 S. Jammi, S. Sakthivel, L. Rout, T. Mukherjee, S. Mandal, R. Mitra, P. Saha and T. Punniyamurthy, *J. Org. Chem.*, 2009, **74**, 1971–1976.

27 H. Rao, Y. Jin, H. Fu, Y. Jiang and Y. Zhao, *Chem.–Eur. J.*, 2006, **12**, 3636–3646.

28 A. Y. Cheng and J. C. Hsieh, *Tetrahedron Lett.*, 2012, **53**, 71–75.

29 X. Lv and W. Bao, *J. Org. Chem.*, 2007, **72**, 3863–3867.

30 S. M. Islam, S. Mondal, P. Mondal, A. S. Roy. K. Tuhina, N. Salam and M. Mobarak, *J. Organomet. Chem.*, 2012, **696**, 4264–4274.

31 R. Zhang, J. Liu, S. Wang, J. Niu, C. Xia and W. Sun, *ChemCatChem*, 2011, **3**, 146–149.

32 P. Ling, D. Li and X. Wang, *J. Mol. Catal. A: Chem.*, 2012, **357**, 112–116.